How Thermal Energy Storage Enhances the Economic Viability of Concentrating Solar Power

Seyed Hossein Madaeni, *Student Member, IEEE,* Ramteen Sioshansi, *Member, IEEE,* and Paul Denholm, *Member, IEEE*

***Abstract*—This paper examines the economic performance and rationale of concentrating solar power (CSP) with and without thermal energy storage (TES). We demonstrate that TES can increase the energy and capacity value of CSP and also show that adding TES to a CSP plant can increase its economic viability by increasing its operating revenues to the point that the capital cost of CSP can be justified.**

***Index Terms*—Capacity value, concentrating solar power, energy economics, thermal energy storage**

I. Introduction

ALTHOUGH the world has recently seen increased interest in renewable sources of electricity, significant challenges still remain for system operators (SOs) in integrating massive amounts of variable renewables (such as wind and solar) into power systems. Many of these issues stem from the uncertain and non-dispatchable nature of such generation. These characteristics can make it difficult to rely on renewables for capacity- or energy-related services.

From a long-term capacity planning standpoint, the variability and non-dispatchability of renewables will typically result in renewables having capacity values significantly lower than nameplate power capacity. This has been demonstrated for both wind [1]–[5] and photovoltaic (PV) solar [6] generation. The variable and uncertain nature of renewables can introduce capacity problems on a short-term basis as well, since these characteristics may require the SO to procure greater amounts of ancillary services (AS) in order to ensure system stability and reliability [7]–[9]. This capacity procurement can increase system operations costs, since more conventional generating capacity will have to be online providing AS.

From an energy service standpoint, uncertain real-time renewable availability can increase system dispatch costs if suboptimal commitment decisions are made day- and hour-ahead using incorrect renewable forecasts [10]–[13]. Renewable non-dispatchability can also raise issues, since the real-time availability of some renewables may not be coincident with electricity demand, reducing the value of renewable energy [14]–[16]. The lack of correlation between loads and renewable availability can also lead to cases, with high renewable penetrations, in which renewable generation must be curtailed due to limited ramping and minimum-load flexibility of conventional generators [17], [18].

Energy storage is often suggested as a potential solution to overcome these and other renewable integration challenges. Using storage in conjunction with a renewable generator can make the renewable plant more dispatchable, while reducing variability and uncertainty of real-time net generation. This is because storage can be used to store excess energy and discharged to supplement renewable output [19], [20]. Storage can reduce the need to use conventional generation for shorter-term AS as well [21], [22]. Since many storage technologies can provide these types of reserves at zero cost (*i.e.* they do not have to be spinning and burning fuel, as many fossil-fueled generators do), this can reduce renewable-related reserve costs. Similarly, storage can reduce the need to deploy high marginal-cost generators in the event of a drop in renewable output.

Although storage can play these and other roles,[1] it is not without its issues. For one, many storage technologies are presently too costly to be economic investments, despite the value of these services [24]–[26]. Another is that many storage technologies incur non-trivial roundtrip efficiency losses when energy is stored and subsequently discharged [24]. This is because most technologies store electricity in a mechanical or chemical medium. The conversion of electricity to and from these other forms of energy often incur significant energy losses.

Concentrating solar power (CSP) is unique among renewable energy generators in that it is variable like solar and wind, but can easily be coupled with thermal energy storage (TES), making it highly dispatchable. This is because, unlike PV, which converts solar radiation directly into electric energy using the photovoltaic effect, CSP uses solar thermal energy to drive a heat engine. By coupling TES with a CSP plant, the thermal energy can be stored for later use, as opposed to it being immediately used to drive the heat engine. TES has several advantages when compared to mechanical or chemical storage technologies. TES generally has low capital costs compared to other storage technologies, as well as very high operating efficiencies. A recent estimate of the cost of adding TES to a CSP plant ranges between $72 and $240 per kWh of electric storage capacity [27] and TES systems that have been incorporated into CSP plants have demonstrated high roundtrip efficiencies, often in excess of 98% [28], [29]. This can be compared to the cost of electrochemical batteries,

This work was supported by the Alliance for Sustainable Energy, LLC under subcontracts AXL-9-99214-01 and AGJ-0-40267-01.

S. Madaeni and R. Sioshansi are with the Integrated Systems Engineering Department, The Ohio State University, Columbus, OH 43210, USA.

P. Denholm is with the Strategic Energy Analysis Center, National Renewable Energy Laboratory, Golden, CO 80401, USA.

[1] See [23] for a comprehensive list of potential renewable- and non renewable-related storage applications.

which are typically over $300 per kWh (not including the expensive power conversion equipment) and have much lower efficiencies [30]. The significantly higher efficiency of TES is because the thermal energy does not have to go through a conversion process to be stored or discharged. Rather, heat exchangers are used to transfer the thermal energy between the heat transfer fluid (HTF) of the CSP plant and the storage system. However, TES can only be used to store thermal energy from the CSP plant, and cannot store electric energy from the rest of the power system.[2]

Despite these limitations on TES, it is a promising technology that can significantly increase the economic viability of CSP by improving its ability to provide capacity- and energy-related services. This paper surveys recent analyses of the economics of CSP and TES, and presents newer results that further demonstrate these benefits and synergies. The remainder of this paper is organized as follows. Section II further describes CSP and TES technologies and the configuration of CSP plants. Section III presents a general modeling framework that can be used to assess the benefits and value of CSP and TES. Section IV summarizes findings regarding CSP and TES revenues, while section V discusses the implications of these findings on the longer-term economic viability of these technologies. Section VI concludes.

II. Description of CSP and TES Technologies

CSP uses a heat engine to convert thermal solar energy into electricity. Three currently deployed CSP designs are parabolic troughs, power towers, and linear Fresnel reflectors [31]–[33]. These designs use a large field of lenses or mirrors to concentrate solar energy onto an HTF. This HTF is used to drive a steam turbine, which is shared by all of the concentrators. Another more modular CSP design is a Stirling dish. This design consists of a Stirling engine mounted onto the end of a dish-shaped concentrator. While some Stirling dish manufacturers are investigating incorporating storage into their designs,[3] no commercial systems have been deployed making cost and performance estimates unreliable. Thus this analysis and discussion does not focus on the Stirling dish technology. Our analyses of CSP and TES values assume a parabolic trough system, although the modeling and analytical framework can easily be generalized to a tower or linear Fresnel reflector system due to similarities in the operation and behavior of the technologies.

TES can be incorporated between the solar field and steam turbine of a trough or tower CSP system, allowing solar thermal energy to be stored for later use. One TES design is a two-tank indirect system [28], [34], [35]. This system consists of two storage tanks (one hot and the other cold), a series of heat exchangers, and a storage fluid, which is typically a molten salt. When energy is being stored, the HTF flows through the heat exchangers and the salt flows from the cold to the hot tank while being heated by the HTF. When energy is discharged from storage, the system operates in reverse and the salt is used to heat the HTF. An advanced TES option is an indirect single-tank thermocline system [36], [37]. This design also uses a storage fluid although the hot and cold fluid are kept in a single tank—the hot and cold fluid remain segregated within the tank due to differences in their densities. This design also allows a low-cost filler material, such as quartzite rock, to replace much of the storage fluid in the tank. Thus a single-tank system can significantly reduce capital costs compared to a two-tank system, due to only one tank and less storage fluid being needed. Relatively large TES systems, which can be charged and discharged for multiple hours at full power, have been built and tested, showing the technology to be viable for large-scale applications [28], [29].

When TES is incorporated into a CSP plant, there are typically three sizing decisions that must be made. This is because the CSP plant consists of three separate but interrelated parts—the steam turbine (which will also be referred to as the powerblock, hereafter), solar field, and TES system. The size of the powerblock is determined by its rated output capacity (MW-e). The size of the solar field is typically measured either by its area or using the concept of a solar multiple (SM), which normalizes the solar field size based on the powerblock size [38]. A solar field with an SM of one is sized to provide sufficient thermal solar energy to operate the powerblock at its rated capacity under reference conditions. A solar field with a different SM will be scaled in proportion to a field with an SM of one (*i.e*. a solar field with an SM of 1.6 will cover an area 1.6 times as large as a solar field with an SM of one). The size of the TES is generally determined by its rated power and energy capacities. We assume that the power capacity of the TES is set to allow the powerblock to operate at its rated power capacity using energy from TES only. The energy capacity of the TES is typically measured in either MWh of thermal energy (MWh-t) that can be stored in the TES system, or by the number of hours of storage. We use the latter convention, and define hours of storage as the number of hours that the TES can be charged at maximum capacity. Due to the extremely high roundtrip efficiencies of TES systems, the number of hours of charging and discharging will be quite close to one another.

The sizing of these components will generally be a nontrivial issue, since the relative sizes of the solar field, powerblock, and TES will determine the capacity factor and utilization of the CSP plant. For instance, a smaller solar field will typically result in many (daytime) hours during which the powerblock is not fully utilized. As the solar field size is increased, powerblock utilization will rise during these hours, however there may be other hours during which the thermal energy collected by the solar field would overload the powerblock and excess energy must go unused. Introducing TES to the CSP plant can help alleviate these issues, by storing excess energy during such hours, and this is one of the benefits of TES that we examine.

[2]It is feasible to store electric energy from the power system using TES if an inductive or resistive heater is used to convert electricity into thermal energy. However, the roundtrip efficiency of this process would be less than 36%.

[3]For example, the U.S. Department of Energy is currently funding Infinia, a Stirling dish manufacturer, to incorporate storage into their Stirling dish systems. See http://eere.energy.gov/solar/pdfs/storage_award_progress_seia.pdf for the project announcement.

III. CSP MODEL

In studying the value of CSP and TES, we represent its operational performance using the mixed-integer programming (MIP) model developed by Sioshansi and Denholm [39], [40]. This model takes the characteristics of the CSP plant (*e.g.* location, powerblock efficiency, TES efficiency, parasitic load of components), weather conditions (including solar insolation and ambient temperature), and size of the CSP plant as fixed. These are combined with market data, such as energy prices, to optimize the operation of the CSP plant to maximize energy revenues. Throughout this analysis we assume the CSP plant to be a price-taker with fixed energy prices that do not respond to energy sales or other decisions made by the CSP plant. Since this analysis is based on a single CSP plant, this price-taking assumption is reasonable because the CSP plant would at most have a marginal effect on the rest of the power system. All modeling and analyses are conducted at hourly timescales. This is because hourly is a sufficiently 'fine' timescale to capture variations in market and weather conditions. Although subhourly variations in solar insolation will affect minute-to-minute output of a CSP plant, the HTF typically has sufficient thermal inertia to keep the powerblock operating through brief subhourly cloud cover [41].

We model CSP plants at two locations in the southwestern U.S., which are listed in Table I, and examine CSP operations and values over the eight years from 1998 to 2005.[4] The locations of these CSP plants are not optimized in any way—rather sites with relatively high solar resources are chosen.[5] The table also specifies what energy price data is used in optimizing the dispatch of the CSP plant at each location. The California ISO (CAISO) market clearing price of energy for the SP15 zone is used for the CSP plant in California (which is located in southern California). Load lambda (LL) data for Nevada Power are used for the CSP plant in Nevada. The LL data are obtained from Form 714 filings with the Federal Energy Regulatory Commission (FERC).

TABLE I: Location of CSP Plants Studied

CSP Site	Coordinates	Energy Price Data
Death Valley California	36.03° N, 117.45° W	CAISO SP15
Nevada	36.55° N, 116.45° W	Nevada Power LL

Our model is developed in two parts. The first part uses the Solar Advisor Model (SAM) [38]. SAM is a software platform, based on the TRNSYS time-series simulation program [42], that simulates the dynamics of a CSP plant. SAM has been validated against empirical CSP data from the Solar Energy Generating Systems [43]. Weather data and solar field characteristics are input to SAM to determine how much thermal energy (MWh-t) is collected by the solar field in each hour, which is denoted by e_t^{SF}.[6] Hourly weather data from the National Solar Radiation Data Base are used as inputs to SAM.[7]

The hourly thermal energy collected by the solar field, as determined by SAM, is then used as an input to the second part of the model. This MIP-based model determines how much thermal energy to deliver to the powerblock and TES, to maximize CSP revenues. The formulation of the model is as follows:

$$\max \sum_{t \in T} (M_t^e - c) \cdot e_t, \quad (1)$$

$$\text{s.t.} \quad l_t = \rho \cdot l_{t-1} + s_t - d_t, \quad \text{// flow balance} \quad (2)$$

$$0 \le l_t \le \eta \cdot \bar{s}, \quad \text{// TES energy limit} \quad (3)$$

$$0 \le s_t \le \bar{s}, \quad \text{// TES charge limit} \quad (4)$$

$$0 \le d_t \le \bar{d}, \quad \text{// TES discharge limit} \quad (5)$$

$$s_t - \phi \cdot d_t + \tau_t + e^{SU} \cdot r_t \le e_t^{SF}, \quad \text{// thermal energy limit} \quad (6)$$

$$e_t = f(\tau_t) - P_h(d_t) - P_b(\tau_t), \quad \text{// net generation} \quad (7)$$

$$\tau^- \cdot u_t \le \tau_t \le \tau^+ \cdot u_t, \quad \text{// powerblock capacity} \quad (8)$$

$$r_t \ge u_t - u_{t-1}, \quad \text{// startup definition} \quad (9)$$

$$u_t \ge \sum_{j=t-\bar{u}}^{t} r_j, \quad \text{// minimum up time} \quad (10)$$

$$u_t, r_t \in \{0, 1\}; \quad \text{// integrality} \quad (11)$$

where we define the following model parameters:

- T set of hours in optimization horizon,
- $\bar{s}$ charging power capacity of TES (MW-t),
- $\bar{d}$ discharging power capacity of TES (MW-t),
- η hours of storage,
- ρ hourly TES energy losses (%),
- ϕ roundtrip TES efficiency (%),
- τ^- minimum operating level of powerblock (MWh-t),
- τ^+ maximum operating level of powerblock (MWh-t),
- e^{SU} powerblock startup energy (MWh-t),
- $\bar{u}$ powerblock minimum up time,
- $f(\cdot)$ powerblock heat rate function,
- $P_h(\cdot)$ HTF pump parastic function,
- $P_b(\cdot)$ powerblock parasitic function,
- c variable generation cost (\$/MWh-e),
- M_t^e price of energy in hour t (\$/MWh-e);

and the following decision variables:

- l_t storage level of TES at the end of hour t (MWh-t)
- s_t energy put into TES in hour t (MWh-t)
- d_t energy taken out of TES in hour t (MWh-t)
- τ_t energy put into powerblock in hour t (MWh-t)
- e_t electric energy sold in hour t (MWh-e)

[4] Our analysis includes two other sites in the southwestern U.S. Results for these sites are not reported here in the interest of brevity and because of similarity to the results reported.

[5] Solar resource maps for the U.S. are publicly available for download at http://www.nrel.gov/gis/solar.html.

[6] A natural question is why we do not use SAM to model the operation of the entire CSP plant. This is because although SAM models the dynamics of a CSP plant, it does not optimize CSP and TES operations as our model does. Instead SAM uses heuristic dispatch rules to determine these decisions. As such, SAM is only able to capture between 87% and 94% of the energy revenues that are possible with our optimization model.

[7] The National Solar Radiation Data Base is available for download at http://rredc.nrel.gov/solar/old_data/nsrdb/.

u_t binary variable indicating powerblock is up (if equal to 1) in hour t

r_t binary variable indicating powerblock is started (if equal to 1) in hour t

Objective function (1) maximizes net revenues, consisting of revenues earned for energy sold less operating costs. Constraint (2) is a flow-balance constraint, which defines the storage level at the end of hour t as a function of the storage level at the end of the hour $t-1$ and the hour-t charging and discharging decisions. The term, ρ, which multiplies the storage level in hour $t-1$, captures heat losses that will naturally occur within the storage tank. We assume hourly heat losses of 0.031%, based on tests conducted at the Solar Two CSP plant in California [29], [44]. Constraints (3) through (5) impose energy and power restrictions on TES charging and discharging. We assume throughout that the TES system begins without any energy in storage at the beginning of the optimization period. It also bears mentioning that by setting the parameter $\eta = 0$, the same MIP can be used to model the operations of a CSP plant without TES.

Constraint (6) limits the total amount of thermal energy used in the CSP plant (consisting of the sum of energy delivered to the powerblock and net energy delivered to TES) to be no greater than the energy collected by the solar field. The term, ϕ, captures roundtrip efficiency losses from energy that is put through the storage cycle, and we assume 1.5% losses [39], [40]. Constraint (7) equates net electricity sold by the CSP plant to net electricity production. The function, $f(\cdot)$, is a heat rate function, which captures the efficiency of the powerblock in converting thermal energy into electricity. The function, $P_h(\cdot)$, captures parasitic energy consumed by the HTF pump, which is used when discharging TES, while the function, $P_b(\cdot)$, captures powerblock parasitics. These functions are approximated as being piecewise-linear, in order to maintain linearity of the MIP [39]. Constraint (8) imposes power capacity restrictions when the powerblock is online. Constraint (9) defines the powerblock startup variable in terms of the commitment variables, while constraint (10) imposes the minimum up-time requirement on the powerblock. Constraint (11) imposes integrality restrictions on the commitment and startup variables.

Because the solar field and TES are sized relative to the powerblock, we hold the power capacity of the powerblock fixed and study the impacts of different TES and solar field sizes. Unless otherwise noted, the CSP plant's characteristics are based on the baseline CSP system modeled in SAM. This plant has a wet-cooled powerblock with a design capacity of 110 MW-e and a two-tank TES system. Although the powerblock has a design capacity of 110 MW-e, it can operate at up to 115% of this design point (giving a maximum output of about 120 MW-e, net of parasitic loads).

Although we examine the value of CSP and TES over multiple years, we simplify the model by using a rolling optimization scheme. This scheme optimizes the dispatch of the plant 24 hours at a time using a 48-hour optimization horizon. The use of the 48-hour optimization horizon allows the CSP plant to keep energy in storage at the end of each day, since it may have value the following day [25]. The revenue of the CSP plant is relatively insensitive to longer optimization horizons [39], [40]. We also assume that the CSP plant has perfect foresight of future weather conditions and energy prices. Although this assumption can overstate the revenues that can actually be captured if price and solar forecasts have to be used, it has been shown that very simple heuristic techniques can capture more than 90% of the revenues possible with perfect foresight of these parameters [25], [26], [39], [40].

IV. Value of CSP and TES

Our analysis focus on three sources of value for a CSP plant: revenues from energy generated and sold by the plant, revenues from AS sold by the plant, and the capacity value of the plant to the power system. We also examine the impacts of different CSP plant configurations, by varying the solar field and TES sizes, on the value of these services.

A. Energy Value of CSP and TES

Fig. 1 summarizes the annual energy revenues, as defined by equation (1), of different-size CSP plants, averaged over the eight years studied. Energy revenues are inflated and given in 2005 dollars, based on the consumer price index (CPI), as reported by the U.S. Department of Labor's Bureau of Labor Statistics. There is considerable interannual variability in revenues, with up to a five-fold difference between the highest- and lowest-value years. The higher energy revenues at the Death Valley location are primarily due to higher energy prices in California (compared to other areas in the southwestern U.S.) [39], [40].

The figures show that increasing either the solar field or TES size will increase CSP revenues, but TES has a greater impact between the two. For instance, increasing the solar field of a CSP plant without TES from an SM of 1.5 to 2.7 will increase revenues by 15% to 28% at the different locations. On the other hand, adding 12 hours of TES to a CSP plant with an SM of 1.5 increases revenues by between 35% and 44%. Moreover, increasing the TES and solar field size together have a superadditive effect. For instance, there is between a 96% and 113% revenue increase between a CSP plant with an SM of 1.5 and no TES and one with an SM of 2.7 and 12 hours of TES.

Adding TES to a CSP plant increases energy revenues in two ways [39], [40]. One is that it allows thermal energy to be stored and used later, when energy prices are higher. This is valuable because high energy prices and solar output are not always coincident. Fig. 2 demonstrates this on a winter day, which will typically have morning and evening price peaks due to heating and lighting loads. The figure shows the dispatch of a CSP plant at the Nevada location with an SM of 2.2 and 12 hours of TES on 5 January, 2001. The figure shows that the output of the solar field peaks midday (around 10 am), whereas energy prices peak in the morning and evening (between 6 am and 7 am in the morning and at 7 pm in the evening). On the day shown in the figure, TES is used to store most of the energy collected by the solar field midday and to shift this generation to the evening when solar field output drops to zero but energy prices rise due to increasing demand.

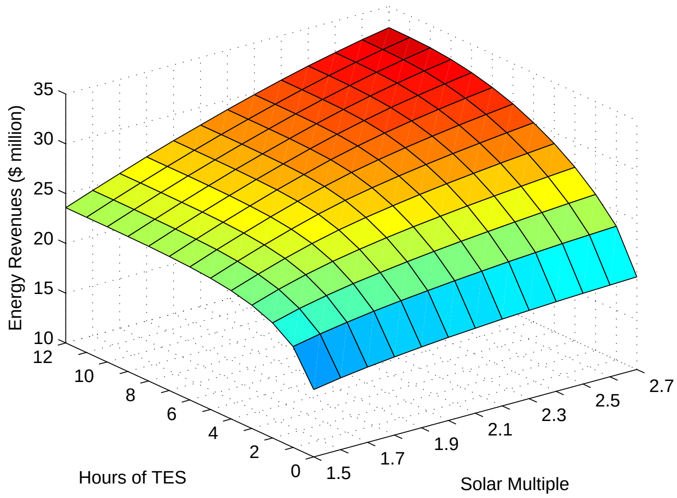

(a) Death Valley.

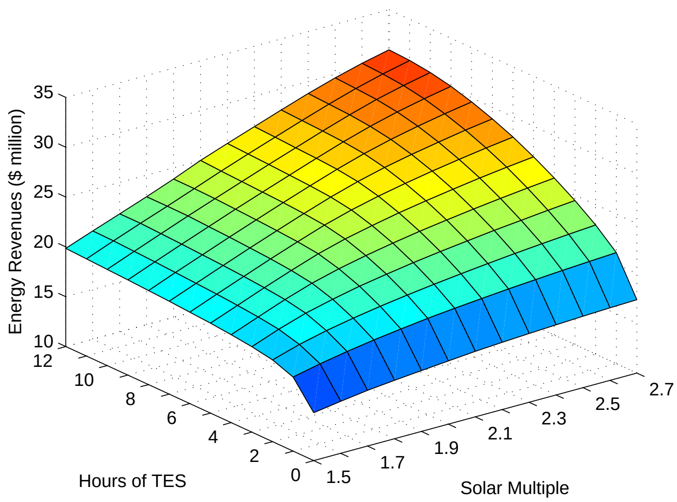

(b) Nevada.

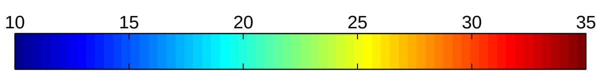

Fig. 1: Average annual energy revenues (2005 $) of a CSP plant at the Death Valley and Nevada locations.

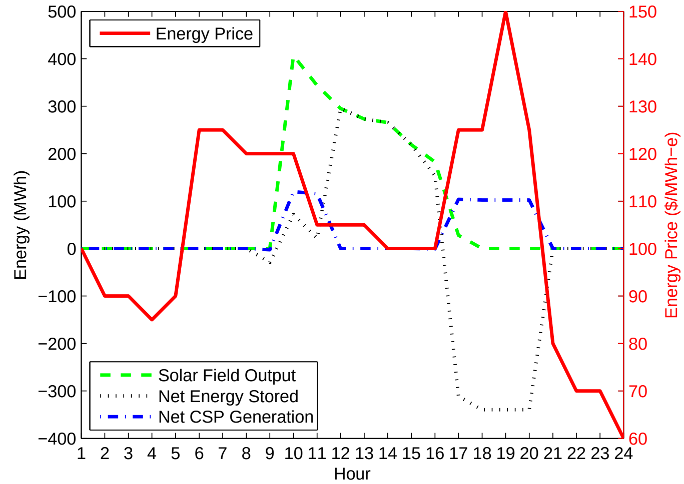

Fig. 2: Dispatch of a CSP plant at Nevada location with an SM of 2.2 and 12 hours of TES on 5 January, 2001.

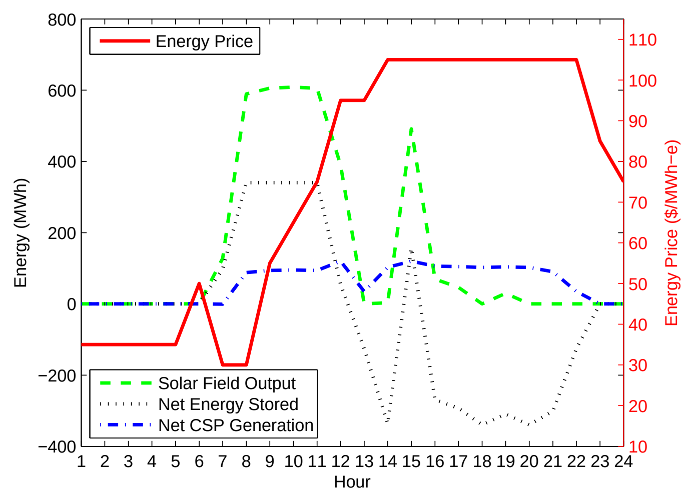

Fig. 3: Dispatch of a CSP plant at Nevada location with an SM of 2.2 and 12 hours of TES on 20 June, 2001.

Fig. 3, which shows the dispatch of the same CSP plant on 20 June, 2001, demonstrates similar use of TES during the summer. Diurnal load patterns are different in the summer than in the winter, since electricity is used for midday and afternoon cooling. As such, solar output and generating loads will tend to be more coincident than in the winter. Due to thermal inertia in buildings, however, cooling loads and associated high electricity prices can lag solar output by an hour or more. Fig. 3 demonstrates these relationships by showing an afternoon electricity price peak beginning at 2 pm which is shortly after the peak in solar output at 10 am. In this case, TES increases energy revenues by allowing solar energy to be stored midday and discharged later during the load and price peak. Fig. 3 also demonstrates that TES can be used to operate the powerblock during brief reductions in solar resource, which occurs between 1 and 2 pm due to prolonged cloud cover. Although a solar resource pattern of this type is relatively atypical, this demonstrates the important ability of TES to keep the plant running during a short midday reduction in solar radiation.

Figs. 2 and 3 also point to another benefit that TES provides, which is that it allows excess energy collected by the solar field (that would overload the powerblock) to be stored for later use. For instance, Fig. 2 shows that at 10 am the solar field collects about 407 MWh-t of solar energy. Of this 335 MWh-t is put into the powerblock, which fully loads it. The remaining 72 MWh-t is put into storage for later use. Similar behavior is also observed at noon and later at 3 pm on 20 June, 2001, when the powerblock is fully loaded and excess solar energy is put into storage.

Fig. 4 summarizes these two benefits of TES for a CSP plant at the Nevada location with an SM of 2.0. It shows the average selling price of electricity generated by the CSP plant, as well as unused solar field energy (*i.e.* energy that is not put into TES or the powerblock and is instead lost) as a function of hours of TES. The selling price is averaged over the eight years modeled. The wasted energy is an annual average over the eight years, and is given as a percentage of the 1,243 GWh-t of energy that the solar field collects on average each year. The figure shows that as the TES size increases, the average selling price of CSP generation increases, since the plant has more flexibility to shift solar energy to higher-priced hours. Similarly, increasing the TES size allows more solar field energy to be used, with less than 1% of the solar field energy wasted with six or more hours of storage. There is, however, still some unused energy even with 12 hours of storage, showing that there are consecutive periods with extremely high solar output that cannot be used.

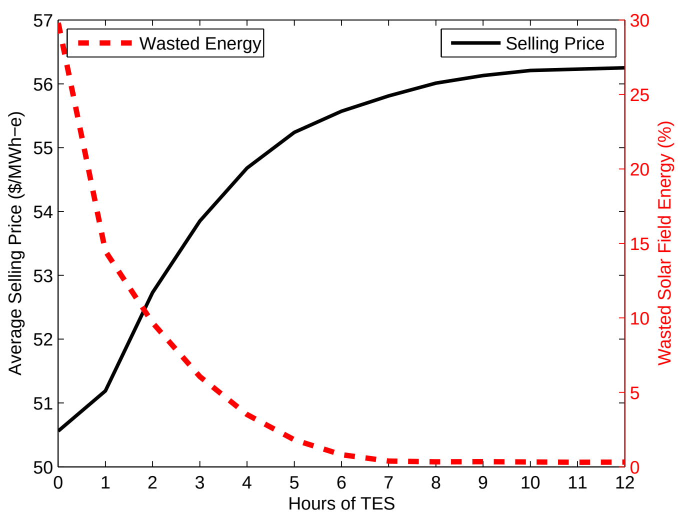

Fig. 4: Average selling price of electricity from CSP plant and average annual unused solar field energy for a CSP plant at the Nevada location with an SM of 2.0.

Depending on the size of the solar field, TES provides these two benefits to varying extents. For instance, adding 12 hours of TES to a CSP plant with an SM of 1.5 at the Nevada location will increase the average selling price of energy from $58.70 to $67.51, while allowing an additional 162 GWh of solar field energy to be used annually. Adding 12 hours of TES to a CSP plant at the same location with an SM of 2.7 will, on the other hand, increase the selling price from $57.99 to $60.36 while allowing an additional 662 GWh to be used. These differences also demonstrate that these two uses of TES 'compete' with one another. This is because using TES to increase the selling price of the CSP plant's output forces energy to be kept in storage until energy prices rise. Keeping energy in TES reduces the ability to store excess solar field energy, however, since TES must discharged to allow excess energy in subsequent hours to then be stored.

The use of TES to allow more solar field energy to be used also points to the added flexibility that TES offers in sizing a CSP plant. This is because when TES is added, more energy produced by a solar field that is oversized relative to the powerblock can be used. Depending on the costs of the solar field, powerblock, and TES components, this can be an attractive option, which can improve the economic rationale of CSP. These issues are discussed at greater length in section V

B. AS Value of CSP and TES

When the CSP plant has the option of providing AS, it must co-optimize AS and energy sales. We use the same basic model, given by (1) through (11), but change the objective function and add constraints and variables to reflect the fact that AS and energy sales are being co-optimized. We assume in this analysis that the CSP plant only provides spinning reserves. Moreover, we assume that the ramping rate of the CSP plant limits it to only providing up to 50% of its nameplate capacity in spinning reserves. Depending on the actual ramp rates and AS qualifications of the plant, these assumptions may over- or understate AS revenues [39], [40].[8]

We model the case with spinning reserves by adding to the model the variables, n_t, which represent how many MW-h-e[9] of spinning reserves the CSP plant provides in each hour. We also add variables l_t^n, d_t^n, τ_t^n, and e_t^n, which capture how the CSP plant would be operated if the spinning reserves sold by the CSP plant are called by the SO in real-time (these variables represent the ending storage level of TES, energy taken out of TES, energy put into the powerblock, and generation of the CSP plant in hour t, respectively, if hour-t spinning reserves are called). These variables are included, with accompanying constraints, to ensure that the CSP plant is able to provide energy if its spinning reserves are called in real-time. We assume that the CSP plant must only provide called spinning reserves for a single hour. Moreover, we do not include any costs or revenues associated with ancillary services that are called in real-time, and only include revenues from making reserve capacity available. These assumptions are justified by the fact that spinning reserves are seldom called in real-time [46].

The formulation of the model that co-optimizes energy and spinning reserve sales is given by:

$$\max \sum_{t \in T} [(M_t^e - c) \cdot e_t + M_t^n \cdot n_t], \tag{12}$$

$$\text{s.t. } (2) - (11), \tag{13}$$

$$0 \le n_t \le \sigma \cdot f(\tau^+), \quad \text{// AS limit} \tag{14}$$

$$e_t + n_t = e_t^n, \quad \text{// AS call met} \tag{15}$$

$$l_t^n = \rho \cdot l_{t-1} + s_t - d_t^n, \quad \text{// flow balance} \tag{16}$$

$$0 \le l_t^n \le \eta \cdot \bar{s}, \quad \text{// TES energy limit} \tag{17}$$

$$0 \le d_t^n \le \bar{d}, \quad \text{// TES discharge limit} \tag{18}$$

$$s_t - \phi \cdot d_t^n + \tau_t^n + e^{SU} \cdot r_t \le e_t^{SF}, \quad \text{// thermal energy limit} \tag{19}$$

$$e_t^n = f(\tau_t^n) - P_h(d_t^n) - P_b(\tau_t^n), \quad \text{// net generation} \tag{20}$$

$$\tau^- \cdot u_t \le \tau_t^n \le \tau^+ \cdot u_t; \quad \text{// powerblock capacity} \tag{21}$$

[8]For example, an estimate of AS revenues for battery energy storage suggests that regulation services provide much higher potential revenues than spinning reserves [45].

[9]We use the unit, MW-h-e, which represents a MW of electric capacity provided for an hour, to measure AS sales. This should be contrasted with a MWh-e, which is a unit of electric energy and represents a MW of power provided for an hour.

where we define the parameters:

M_t^n price of spinning reserves in hour t ($/MW-h-e),

σ maximum spinning reserves capacity (% of nameplate capacity).

Objective function (12) maximizes the sum of energy and spinning reserve revenues. Constraints (2) through (11) impose the same restrictions as before on TES, thermal energy collected by the solar field, and relations giving net generation in terms of the heat rate function and component parasitics. Constraint (14) limits spinning reserve sales in each hour based on the ramping capability of the powerblock. Constraints (15) through (21) model the operation of the CSP plant if the spinning reserves are called in real-time, and ensure that the plant can serve such a call. Constraint (15) ensures that net CSP generation if spinning reserves are called (e_t^n) equal the sum of energy and spinning reserve sales ($e_t + n_t$), while the remaining constraints ensure that e_t^n MWh-e can be feasibly generated by the CSP plant in such an instance.

Because AS price or cost data for Nevada Power are not available, we model the case with spinning reserves for the Death Valley location only. We use historical hourly spinning reserve price data for the CAISO's SP15 zone. Moreover, because the CAISO only has data starting from 2001 available, we only model the five years 2001 through 2005.

Fig. 5 summarizes average annual AS revenues for the Death Valley plant. AS revenue is defined as the incremental increase in the objective function value between the cases in which the CSP plant can and cannot provide AS (*i.e*. the difference in the optimized value of (12) and (1)). These revenues are inflated to 2005 dollars using CPI data. The figure shows that adding AS can yield noticeable revenue increases—with average annual revenues increasing by up to 17%—depending on the size of the CSP plant. Allowing the CSP plant to sell AS can affect the dispatch of the plant [39], [40]. In some cases the CSP plant will produce less energy, thereby diverting thermal energy collected by the solar field to TES in order to increase the amount of AS it can provide. In others the powerblock will be started up when it otherwise wouldn't be if the CSP plant could only sell energy, in order to take advantage of favorable AS prices.

Fig. 5 shows that AS revenues are increasing in the size of TES. It also shows that AS revenues are highest for a CSP plant with a small solar field but large TES capacity. This is because a plant with such a configuration will use TES less to store excess energy collected by the solar field, meaning that there is greater flexibility in keeping energy in storage to provide AS.

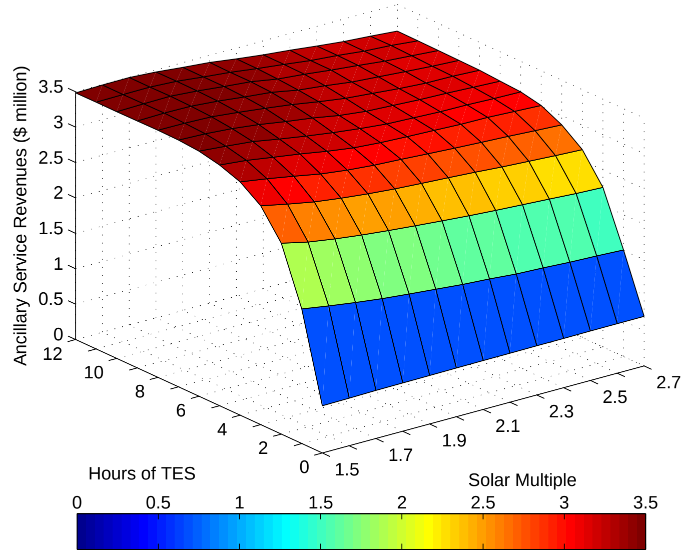

Fig. 5: Average annual ancillary service revenues (2005 $) of a CSP plant at the Death Valley location.

C. *Capacity Value of CSP and TES*

Adding TES to a CSP plant can also increase the capacity value of the plant to the power system. This is because energy can be kept in storage for anticipated system shortage events, for instance when high loads are forecasted. In many systems the annual load peaks in the summer, due to cooling needs. As Fig. 3 suggests, these peaks can lag peaks in solar resource, due to thermal inertia in buildings. Thus a CSP plant can have a higher capacity value with TES due to this lack of perfect coincidence between load and solar peaks.

Although some power systems have or are moving toward capacity payments, other systems rely on energy markets only to signal the need for generating capacity [47]. Under an energy-only market design, scarcity pricing drives energy prices higher when loads are close to the generating capacity of the system. These scarcity prices should, in turn, signal generation capacity to enter the market (or loads to fall) during these periods. Since our basic model, consisting of (1) through (11), operates the CSP plant to maximize energy revenues, the simulated operation of the plants is in concert with an energy-only market design. Moreover, the CAISO operated as an energy-only market during our study period. Thus, we can use the simulated operation of the CSP plant, discussed in section IV-A, to estimate the capacity value that the plant would provide the system.

Estimating the capacity value of a CSP plant with TES can be difficult, however. This is because energy in TES could be used to supplement the output of the CSP plant during a system shortage event, if the powerblock is not already operating at its maximum capacity. While our model simulates the actual generation of the CSP plant, it does not directly capture this capability of energy in TES. Moreover, energy storage can be likened to an energy-limited generator, such as a hydroelectric reservoir. As such, energy used in hour t cannot be used in subsequent hours. Thus, TES may not be able to serve multiple consecutive hours with system shortage events.

Tuohy and O'Malley [19] propose a technique to estimate the capacity value of storage. Their technique uses operation data to determine the maximum potential output of the storage system in each hour. They then use this maximum output of storage during hours with either the highest loads or the highest loss of load probabilities (LOLPs) to estimate the capacity value of storage. If, for instance, the storage system can, on average, produce 80 MW-e during the highest-load hours, then they approximate the storage system as having a capacity value of 80 MW-e.

The capacity value of the CSP plant can be computed using this technique based on the results of our model, given by (1) through (11). This is done by first defining the maximum potential thermal energy that can be delivered to the powerblock in each hour as:

$$\tau_t^\mu = \max\left\{0, \min\left\{\tau^+, \right.\right.$$
$$\left.\left. e_t^{SF} + \phi \cdot \min\left\{\bar{d}, \rho \cdot l_{t-1}\right\} - e^{SU} \cdot (1 - u_t)\right\}\right\}. \quad (22)$$

Equation (22) defines the maximum amount of thermal energy that can be delivered to the powerblock as the minimum of the powerblock's capacity and the sum of energy collected by the solar field and energy in TES (with associated energy losses taken into account). Equation (22) further assumes that the powerblock can be started up immediately, in the event of a system shortage event. The following equation then defines the amount of this energy that is taken from TES in each hour as:

$$d_t^\mu = \tau_t^\mu - e_t^{SF}. \quad (23)$$

The maximum potential output of the CSP plant is then given by:

$$e_t^\mu = f(\tau_t^\mu) - P_h(d_t^\mu) - P_b(\tau_t^\mu). \quad (24)$$

We estimate the capacity value of the CSP plant by using the 10 hours in each year with the highest loads, which are weighted by the LOLPs. LOLPs are calculated for the entire Western Electricity Coordinating Council (WECC) region, of which California and Nevada are a part. LOLPs are calculated using load and generator data [48]. WECC load data are obtained from Form 714 filings with FERC. WECC generator data are obtained from Form 860 data filed with the U.S. Department of Energy's Energy Information Administration. The Form 860 data specify the generating capacity, prime mover, and generating fuel of each generator in the WECC. Generator outage rates are estimated using the Generating Availability Data System (GADS), produced by the North American Electric Reliability Corporation. The GADS specifies historical outage rates for generators based on unit type and size.

Fig. 6 summarizes the average annual capacity value of CSP plants at the two locations. The capacity values are given as a percentage of the 120 MW-e maximum capacity of the powerblock. They show that the capacity value is generally increasing in the size of the solar field and TES, although this relationship is not monotone. This is because different CSP plant configurations will yield different operational decisions, and in some cases a larger CSP plant may have less energy in TES during a high-LOLP hour. For example, a CSP plant at the Nevada location with four hours of TES and an SM of 2.2 has a capacity value of 114 MW-e in 1999.[10] The same CSP plant with an SM of 2.7 would have a lower capacity value of only 85 MW-e in 1999. This difference in the capacity value is due to less energy being in the TES of the larger CSP plant on 12 July, which is the day with five of the 10 highest hourly loads of the year. The larger CSP plant has less energy in storage because the larger solar field provides sufficient energy to operate the powerblock above its minimum operating point in the afternoon of the previous day. The smaller solar field of the CSP plant with an SM of 2.2 could not meet this minimum-load constraint, and as such the output of the solar field is stored. As such, the CSP plant with an SM of 2.2 can, on average, generate up to 118 MW-e during the five-highest-LOLP hours on 12 July. The larger CSP plant with an SM of 2.7 can only generate up to an average of 74 MW-e during these hours.

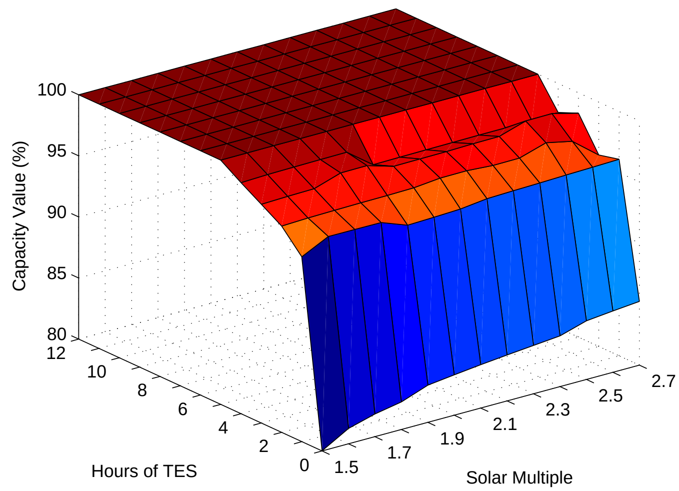

(a) Death Valley.

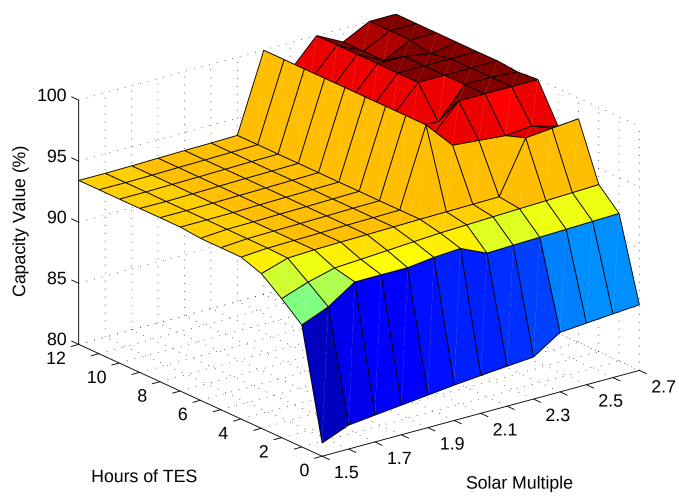

(b) Nevada.

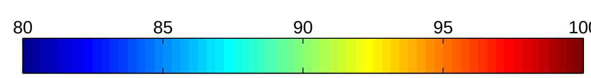

Fig. 6: Average capacity value of a CSP plant at the Death Valley and Nevada locations.

The result that the capacity value of the CSP plant is not monotone in the plant size also points to a potential shortcoming of energy-only markets, in that energy prices will not always be perfectly correlated with loads, LOLPs, and system shortage events. This, in turn, raises the potential need for capacity markets to signal capacity expansion within

[10] We focus on annual capacity values in this discussion since it allows us to more easily explain why the capacity value drops when the SM increases.

a system. If a CSP plant is able to participate in such a capacity market, then the operation of the CSP plant would be adjusted to maximize the sum of energy and capacity payments. This would presumably increase the capacity value of the CSP plant, since most capacity markets include performance requirements, which would incent the CSP plant to have energy available during anticipated system shortages [49]. These performance requirements typically require a generator to be able to provide energy during high-load or low-reserve margin periods. Generators that do not meet these requirements are typically penalized, with penalties often set by the cost of replacement capacity.

V. Overall Economic Performance of CSP and TES

Our analysis thus far has only considered the operating revenues (*i.e.* revenues from energy and AS sales, net of variable operating costs) of a CSP plant that has already been built. We have not examined the broader question of whether an investment in a CSP plant would be economic. This type of an analysis would require estimates of CSP capital costs and multiple years of operating revenues. The cost of utility-scale CSP is still somewhat uncertain due to fluctuations in commodity prices and the potential for substantial manufacturing cost reductions. Furthermore, the cost competitiveness of CSP relative to other generating technologies will depend on future changes in fuel prices and policy decisions, such as carbon regulations.

In light of these and other factors that can affect CSP economics, we opt to use the operating revenues estimated in section IV to compute breakeven costs for the CSP plant. The breakeven cost is defined as the highest capital cost for the CSP plant that can be justified on the basis of a stream of operating revenues. We can also compare these breakeven costs to recent CSP capital cost estimates and targets. Turchi *et al.* [27] give cost estimates for a CSP plant built in 2010, based on current manufacturing and component costs, as well as future cost forecasts for 2020. We break their cost estimates into three components—a solar field cost that is proportional to the SM of the plant, a TES cost that is proportional to the hours of TES, and a fixed cost for the balance of the plant (including the powerblock). Because of major fluctuations in generator capacity costs, we deflate these cost estimates to 2005 dollars using the Chemical Engineering Plant Cost Indices.[11] The cost estimates that we use are summarized in Table II.

TABLE II: CSP Capital Cost Estimates (2005 Dollars) [27]

	Year	
Component	2010	2020
Fixed ($ million)	129.69	129.69
Solar Field ($ million/SM)	216.93	133.00
TES ($ million/hour)	29.25	8.85

In order to estimate a breakeven cost, we must make assumptions regarding the cost of financing a CSP plant, any subsidies for which the plant would be eligible, and what operating revenues the plant would earn. Instead of making detailed CSP financing assumptions, we rely on a capital charge rate (CCR), which converts the total cost of the CSP plant into an annual capital cost that includes all financing-related costs [50]. We assume an 11% CCR, which is typical for the electric power industry. Solar plants are currently eligible for an investment tax credit (ITC) worth 30% of the capital cost of a plant, which we assume the CSP plant is eligible for.

Our analysis assumes that the CSP plant can earn energy and AS revenues, as estimated in section IV. Since we are only able to compute AS revenues for the Death Valley plant, we inflate the energy revenues of a CSP plant at the Nevada location in proportion to the revenue increase of the Death Valley plant when it can provide AS. We further assume that the CSP plant earns revenues associated with its capacity value. Although there were no capacity markets operating in the WECC during the period that we study, a CSP plant would avert the need for a utility or load-serving entity to build generating capacity to meet reliability and capacity requirements. As such, we assume that a utility would be willing to pay, up to the capital cost of a natural gas-fired combustion turbine, for the capacity provided by a CSP plant.[12] We use the cost of a combustion turbine because this is a generation technology typically built to meet incremental capacity requirements, due to its low capital cost. Using the assumed 11% CCR and a recent cost estimate of $625/kW for a combustion turbine (in 2005 dollars) [51] gives a value of $68,750 per MW-e of capacity provided by the CSP plant.

Based on these assumptions, we define the average annual operating profits of the CSP plant, π, as the sum of the optimized value of objective function (12) and the annual capacity value of the plant multiplied by $68,750/MW-e. The breakeven cost of the plant is computed as:

$$B = \frac{\pi}{\gamma^{CCR} \cdot (1 - \gamma^{ITC})}, \tag{25}$$

where B is the breakeven cost and γ^{ITC} and γ^{CCR} represent the ITC rate and CCR.

Fig. 7 summarizes the estimated breakeven cost of CSP plants at the two locations. The breakeven costs are normalized by the 110 MW-e gross nameplate capacity of the CSP plant's powerblock, to give a $/kW cost. The magenta circles in the figure indicate CSP plant configurations that would have 2020 capital costs estimates below their breakeven costs. Such plant configurations would be economic in that capital costs could be recovered from the energy, AS, and capacity revenues that we estimate. No CSP plant configurations are economic with the 2010 cost estimates. The figures show that at both of the locations CSP will be economic with the future costs. Moreover, the plant configurations that are economic all include at least one hour of TES, indicating that the incremental value of adding TES to a CSP plant outweighs its cost and improves the economic rationale of investing in the remainder of the plant.

[11] These indices are available at http://www.che.com/pci/.

[12] Alternately, a utility that builds a CSP plant would derive a cost savings, since the CSP plant would reduce the need for the utility to build additional generating capacity.

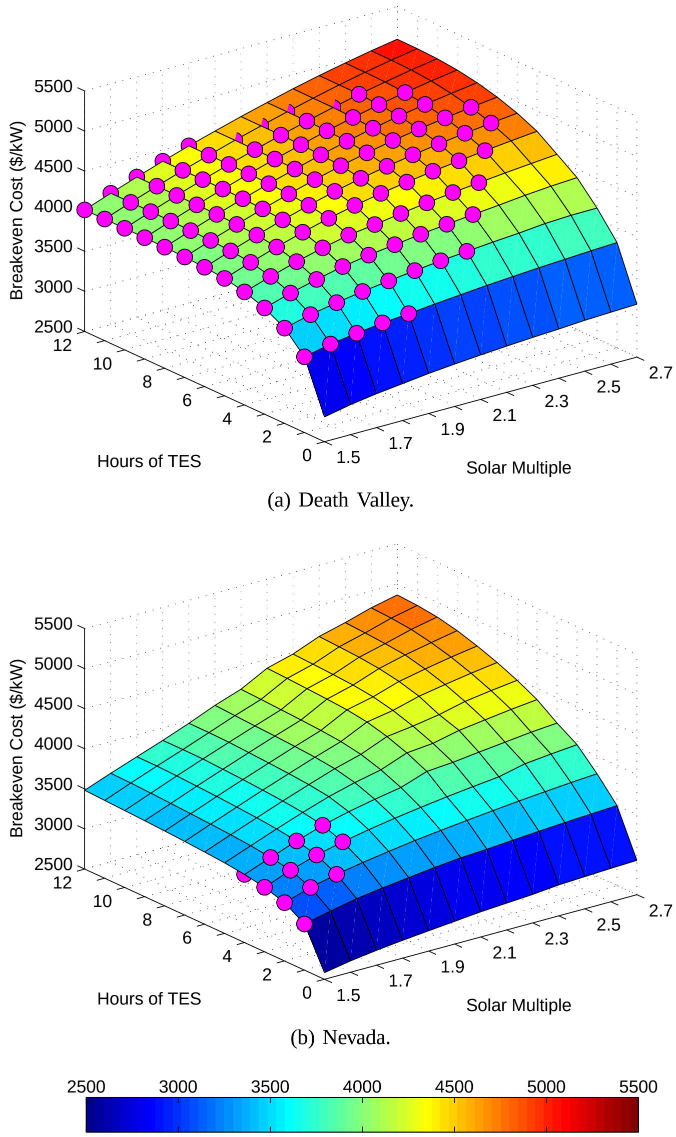

(a) Death Valley.

(b) Nevada.

Fig. 7: Breakeven cost (2005 dollars per kW) of a CSP plant at the Death Valley and Nevada locations. Magenta circles indicate plant configurations that are economic with 2020 CSP capital cost estimates and a 30% ITC.

Our results indicate that with current market conditions and cost projections, two to four hours of TES is more economically optimal compared to the greater number of hours that are often included in CSP analyses (*e.g.* Turchi *et al.* assume six hours as a 'baseline' CSP configuration [27]). Fig. 7b shows that six hours of TES is not economic at the Nevada location with 2020 capital cost estimates. Moreover, a CSP plant with three or four hours of TES maximizes return on investment at the Death Valley location. Continued cost reductions will nevertheless be necessary for CSP to be economically competitive with fossil-fueled generation. The gap would obviously be reduced if CSP were able to take advantage of its carbon or other emissions benefits.

VI. Concluding Remarks

This paper examines the economic rationale of CSP and TES. Using a MIP-based model, we are able to optimize the operation of CSP plants and show the benefits that adding TES provides. Benefits that we examine include increasing energy and AS revenues, as well as the capacity value of the CSP plant. The addition of TES increases the value of energy sold by the CSP plant, and reduces curtailed production, typically increasing overall revenues by at least 35%. Energy revenues constitute most of the operating revenues of the CSP plant. Depending on the location and configuration of the plant, energy revenues account for between 66% and 76% of total revenues, as opposed to between 2% and 7% for AS revenues and between 17% and 32% for capacity payments.

When comparing the operating revenues of the CSP plant to capital cost estimates, we find that under current market conditions, the optimal amount of TES is about two to four hours. However, capital costs for CSP plants will need to be reduced, (probably along with carbon constraints being imposed) for CSP to be competitive with fossil fuel-based generation. As the markets evolve, including changes in the generation mix and increases in wind and other solar generation, the optimal amount of TES may increase. Our analysis uses historical data from power systems which are dominated by fossil-fueled generation. As renewable penetrations rise and these fuels become less prevalent, there will be changes in energy and AS prices, which can affect revenues we estimate and the optimal mix of new generation technologies. The inherent flexibility of CSP technology, especially with TES, can make these plants even more valuable as renewable penetration rises. Further analysis will be needed to evaluate the overall cost competitiveness of CSP compared to wind and PV especially considering their very different performance characteristics.

It is important to stress that this analysis assumes a parabolic trough CSP system. The results and conclusions may be different for other CSP systems, including higher temperature trough systems or power towers. It should also be noted that we do not analyze all of the potential benefits of adding TES to a CSP plant. One is a reduction in CSP integration costs, such as the cost of greater AS requirements or real-time system redispatch due to CSP. Even without TES, CSP integration costs will likely be smaller than wind or PV. This is because of the thermal inertia in the HTF of a CSP plant, which will allow the powerblock to operate during brief cloud cover [41]. As such, a CSP plant will not be as susceptible to a sudden drop in generation as PV or wind may be. When TES is added to a CSP plant, we see that its capacity value and ability to provide AS increase, suggesting that the output of the CSP plant is more firm. However, a more detailed analysis of the system effects of integrating large amounts of CSP with and without TES will be needed to more concretely address this question.

Another benefit that TES could provide is by reducing transmission requirements for a CSP plant that is distant from a load center. In the U.S. and other parts of the world, many of the prime renewable resources are in sparsely populated areas and will require major transmission investments in order to deliver power to consumers [51], [52]. Depending on whether they will be used solely for delivery of renewable energy, the capacity factor of these transmission investments can be quite low, making these investments significantly more expensive on a levelized cost of energy basis. Energy storage that is co-located with a renewable generator can reduce the need for transmission capacity to deliver renewable energy. This is because excess energy that would overload a transmission line can be stored and discharged later, when renewable output falls below the capacity of the line. This has been demonstrated for compressed-air energy storage co-located with wind [50], and could also apply to CSP, although this benefit would be extremely site-specific. Moreover, since some regions of the southwestern U.S. have both solar and wind resources, a wind generator that is co-located with a CSP plant with TES could benefit from such a transmission capacity reduction.

Acknowledgment

The authors would like to thank C. Turchi, M. Mehos, W. Short, R. Newmark, A. Sorooshian, the editors, and five anonymous reviewers for helpful discussions and suggestions. Udi Helman and Darren Lamb of the California ISO and Richard Sobonya of the FERC provided invaluable assistance in gathering CAISO market price and Nevada Power load lambda data.

References

[1] M. R. Milligan, "Measuring wind plant capacity value," National Renewable Energy Laboratory, Tech. Rep. NREL/TP-441-20493, 1996.

[2] M. R. Milligan and B. Parsons, "Comparison and case study of capacity credit algorithms for wind power plants," *Wind Engineering*, vol. 23, pp. 159–166, May 1999.

[3] M. R. Milligan and T. Factor, "Optimizing the geographic distribution of wind plants in iowa for maximum economic benefit and reliability," *Wind Engineering*, vol. 24, pp. 271–290, July 2000.

[4] M. R. Milligan and K. Porter, "The capacity value of wind in the united states: Methods and implementation," *The Electricity Journal*, vol. 19, pp. 91–99, March 2006.

[5] G. R. Pudaruth and F. Li, "Capacity credit evaluation: A literature review," in *Third International Conference on Electric Utility Deregulation and Restructuring and Power Technologies*. Nanjing, China: Institute of Electrical and Electronics Engineers, 6-9 April 2008, pp. 2719–2724.

[6] R. Perez, R. Seals, and R. Stewart, "Assessing the load matching capability of photovoltaics for us utilities based upon satellite-derived insolation data," in *Conference Record of the Twenty Third IEEE Photovoltaic Specialists Conference*. Louisville, KY, USA: Institute of Electrical and Electronics Engineers, 10-14 May 1993, pp. 1146–1151.

[7] S. T. Lee and Z. A. Yamayee, "Load-following and spinning-reserve penalties for intermittent generation," *IEEE Transactions on Power Apparatus and Systems*, vol. PAS-100, pp. 1203–1211, March 1981.

[8] L. Söder, "Reserve margin planning in a wind-hydro-thermal power system," *IEEE Transactions on Power Systems*, vol. 8, pp. 564–571, May 1993.

[9] R. Doherty and M. O'Malley, "A new approach to quantify reserve demand in systems with significant installed wind capacity," *IEEE Transactions on Power Systems*, vol. 20, pp. 587–595, May 2005.

[10] A. Fabbri, T. G. S. Román, J. R. Abbad, and V. H. M. Quezada, "Assessment of the cost associated with wind generation prediction errors in a liberalized electricity market," *IEEE Transactions on Power Systems*, vol. 20, pp. 1440–1446, August 2005.

[11] E. A. DeMeo, W. Grant, M. R. Milligan, and M. J. Schuerger, "Wind plant integration," *IEEE Power and Energy Magazine*, vol. 3, pp. 38–46, November-December 2005.

[12] J. C. Smith, M. R. Milligan, E. A. DeMeo, and B. Parsons, "Utility wind integration and operating impact state of the art," *IEEE Transactions on Power Systems*, vol. 22, pp. 900–908, August 2007.

[13] E. A. DeMeo, G. A. Jordan, C. Kalich, J. King, M. R. Milligan, C. Murley, B. Oakleaf, and M. J. Schuerger, "Accommodating wind's natural behavior," *IEEE Power and Energy Magazine*, vol. 5, pp. 59–67, November-December 2007.

[14] R. J. Green and N. Vasilakos, "Market behaviour with large amounts of intermittent generation," *Energy Policy*, vol. 38, pp. 3211–3220, July 2010.

[15] P. Twomey and K. Neuhoff, "Wind power and market power in competitive markets," *Energy Policy*, vol. 38, pp. 3198–3210, July 2010.

[16] R. Sioshansi, "Increasing the value of wind with energy storage," *The Energy Journal*, vol. 32, pp. 1–30, 2011.

[17] P. Denholm and R. M. Margolis, "Evaluating the limit of solar photovoltaics (PV) in traditional electric power systems," *Energy Policy*, vol. 35, pp. 2852–2861, 2007.

[18] R. Sioshansi and W. Short, "Evaluating the impacts of real-time pricing on the usage of wind generation," *IEEE Transactions on Power Systems*, vol. 24, pp. 516–524, May 2009.

[19] A. Tuohy and M. O'Malley, "Impact of pumped storage on power systems with increasing wind penetration," in *Power & Energy Society General Meeting*. Calgary, AB, Canada: Institute of Electrical and Electronics Engineers, 26-30 July 2009, pp. 1–8.

[20] P. Denholm, E. Ela, B. Kirby, and M. Milligan, "The role of energy storage with renewable electricity generation," National Renewable Energy Laboratory, Tech. Rep. NREL/TP-6A2-47187, January 2010.

[21] J. García-González, R. M. R. de la Muela, L. M. Santos, and A. M. González, "Stochastic joint optimization of wind generation and pumped-storage units in an electricity market," *IEEE Transactions on Power Systems*, vol. 23, pp. 460–468, May 2008.

[22] A. Tuohy, P. Meibom, E. Denny, and M. O'Malley, "Unit commitment for systems with significant wind penetration," *IEEE Transactions on Power Systems*, vol. 24, pp. 592–601, May 2009.

[23] J. Eyer and G. Corey, "Energy storage for the electricity grid: Benefits and market potential assessment guide," Sandia National Laboratories, Tech. Rep. SAND2010-0815, February 2010.

[24] "EPRI-DOE handbook for energy storage for transmission and distribution applications," Electric Power Research Institute and the U.S. Department of Energy, Palo Alto, CA and Washington, DC, USA, Tech. Rep. 1001834, 2003.

[25] R. Sioshansi, P. Denholm, T. Jenkin, and J. Weiss, "Estimating the value of electricity storage in PJM: Arbitrage and some welfare effects," *Energy Economics*, vol. 31, pp. 269–277, March 2009.

[26] R. Sioshansi, P. Denholm, and T. Jenkin, "A comparative analysis of the value of pure and hybrid electricity storage," *Energy Economics*, vol. 33, pp. 56–66, January 2011.

[27] C. Turchi, M. Mehos, C. K. Ho, and G. J. Kolb, "Current and future costs for parabolic trough and power tower systems in the us market," National Renewable Energy Laboratory, Tech. Rep. NREL/CP-5500-49303, October 2010.

[28] U. Herrmann and D. W. Kearney, "Survey of thermal energy storage for parabolic trough power plants," *Journal of Solar Energy Engineering*, vol. 124, pp. 145–152, May 2002.

[29] J. E. Pacheco and R. Gilbert, "Overview of recent results of the solar two test and evaluations program," Sandia National Laboratories, Tech. Rep. SAND99-0091C, January 1999.

[30] D. Rastler, "New demand for energy storage," *Electric Perspectives*, vol. 33, pp. 30–47, September-October 2010.

[31] H. Price, E. Lüpfert, D. Kearney, E. Zarza, G. Cohen, R. Gee, and R. Mahoney, "Advances in parabolic trough solar power technology," *Journal of Solar Energy Engineering*, vol. 124, pp. 109–125, May 2002.

[32] "Assessment of parabolic trough and power tower solar technology cost and performance forecasts," National Renewable Energy Laboratory, Tech. Rep. NREL/SR-550-34440, October 2003.

[33] M. Selig and M. Mertins, "From saturated to superheated direct solar steam generation—technical challenges and economical benefits," in *SolarPACES 2010 Conference*, Perpignan, France, 21-24 September 2010.

[34] D. W. Kearney, B. Kelly, U. Herrmann, R. Cable, J. E. Pacheco, A. R. Mahoney, H. Price, D. M. Blake, P. Nava, and N. Potrovitza, "Engineering aspects of a molten salt heat transfer fluid in a trough solar field," *Energy*, vol. 29, pp. 861–870, April-May 2004.

[35] A. Gil, M. Medrano, I. Martorell, A. Lázaro, P. Dolado, B. Zalba, and L. F. Cabeza, "State of the art on high temperature thermal energy storage for power generation. part 1—concepts, materials and modellization," *Renewable and Sustainable Energy Reviews*, vol. 14, pp. 31–55, January 2010.

[36] J. E. Pacheco, S. K. Showalter, and W. J. Kolb, "Development of a molten-salt thermocline thermal storage system for parabolic trough plants," *Journal of Solar Energy Engineering*, vol. 124, pp. 153–159, May 2002.

[37] D. L. Barth, J. E. Pacheco, W. J. Kolb, and E. E. Rush, "Development of a high-temperature, long-shafted, molten-salt pump for power tower applications," *Journal of Solar Energy Engineering*, vol. 124, pp. 170–175, May 2002.

[38] P. Gilman, N. Blair, M. Mehos, C. Christensen, and S. Janzou, "Solar advisor model user guide for version 2.0," National Renewable Energy Laboratory, Tech. Rep. NREL/TP-670-43704, August 2008.

[39] R. Sioshansi and P. Denholm, "The value of concentrating solar power and thermal energy storage," National Renewable Energy Laboratory, Tech. Rep. NREL/TP-6A2-45833, February 2010.

[40] ——, "The value of concentrating solar power and thermal energy storage," *IEEE Transactions on Sustainable Energy*, vol. 1, pp. 173–183, October 2010.

[41] D. Lew, N. Miller, K. Clark, G. Jordan, and Z. Gao, "Impact of high solar penetration in the western interconnection," National Renewable Energy Laboratory, Tech. Rep. NREL/TP-5500-49667, December 2010.

[42] A. Fiksel, J. W. Thornton, S. A. Klein, and W. A. Beckman, "Developments to the TRNSYS simulation program," *Journal of Solar Energy Engineering*, vol. 117, pp. 123–127, May 1995.

[43] H. Price, "Parabolic trough solar power plant simulation model," National Renewable Energy Laboratory, Tech. Rep. NREL/CP-550-33209, January 2003.

[44] U. Herrmann, B. Kelly, and H. Price, "Two-tank molten salt storage for parabolic trough solar power plants," *Energy*, vol. 29, pp. 883–893, April-May 2004.

[45] J. Tomić and W. Kempton, "Using fleets of electric-drive vehicles for grid support," *Journal of Power Sources*, vol. 168, pp. 459–468, June 2007.

[46] W. Kempton and J. Tomić, "Vehicle-to-grid power fundamentals: Calculating capacity and net revenue," *Journal of Power Sources*, vol. 144, pp. 268–279, June 2005.

[47] D. Finon and V. Pignon, "Capacity mechanisms in imperfect electricity markets," *Utilities Policy*, vol. 16, pp. 141–142, September 2008.

[48] R. Billinton and R. N. Allan, *Reliability Evaluation of Power Systems*. Boston: Pitman Advanced Publishing Program, 1984.

[49] P. Cramton and S. Stoft, "A capacity market that makes sense," *The Electricity Journal*, vol. 18, pp. 43–54, August-September 2005.

[50] P. Denholm and R. Sioshansi, "The value of compressed air energy storage with wind in transmission-constrained electric power systems," *Energy Policy*, vol. 37, pp. 3149–3158, August 2009.

[51] "20% wind energy by 2030: Increasing wind energy's contribution to U.S. electricity supply," U.S. Department of Energy, Tech. Rep. DOE/GO-102008-2567, July 2008.

[52] *Study of Electric Transmission in Conjunction with Energy Storage Technology*, Lower Colorado River Authority, Austin, Texas, August 2003, prepared for Texas State Energy Conservation Office.

Seyed Hossein Madaeni (S'11) is a Ph.D. student in the Integrated Systems Engineering Department at The Ohio State University. His research focuses on renewable energy analysis and restructured power systems. He holds a B.S. and an M.S. in electrical engineering from the University of Tehran.

Ramteen Sioshansi (M'11) is an assistant professor in the Integrated Systems Engineering Department at The Ohio State University. His research focuses on renewable and sustainable energy system analysis and the design of restructured competitive electricity markets.

He holds a B.A. in economics and applied mathematics and an M.S. and Ph.D. in industrial engineering and operations research from the University of California, Berkeley, and an M.Sc. in econometrics and mathematical economics from The London School of Economics and Political Science.

Paul Denholm (M'11) is a senior analyst in the Strategic Energy Analysis Center at the National Renewable Energy Laboratory. His research interests are in the effects of large-scale renewable energy deployment in electric power systems, and renewable energy enabling technologies such as energy storage and long distance transmission.

He holds a B.S. in physics from James Madison University, an M.S. in instrumentation physics from the University of Utah, and a Ph.D. in land resources/energy analysis and policy from the University of Wisconsin-Madison.